

Original Manuscript

Comparative analysis of Ag NPs functionalized with olive leaf extract and oleuropein and toxicity in human trophoblast cells and peripheral blood lymphocytes

Andrea Pirković^{1,*}, Vesna Lazić², Biljana Spremo-Potparević³, Lada Živković³, Dijana Topalović³, Sanja Kuzman², Jelena Antić-Stanković⁴, Dragana Božić⁴, Milica Jovanović Krivokuća¹, Jovan M. Nedeljković²

¹Department for Biology of Reproduction, University of Belgrade, INEP Institute for Application of Nuclear Energy, Belgrade, Serbia

²Centre of Excellence for Photoconversion, Vinča Institute of Nuclear Sciences —National Institute of the Republic of Serbia, University of Belgrade, Belgrade, Serbia

³Department of Pathobiology, Faculty of Pharmacy, University of Belgrade, Belgrade, Serbia

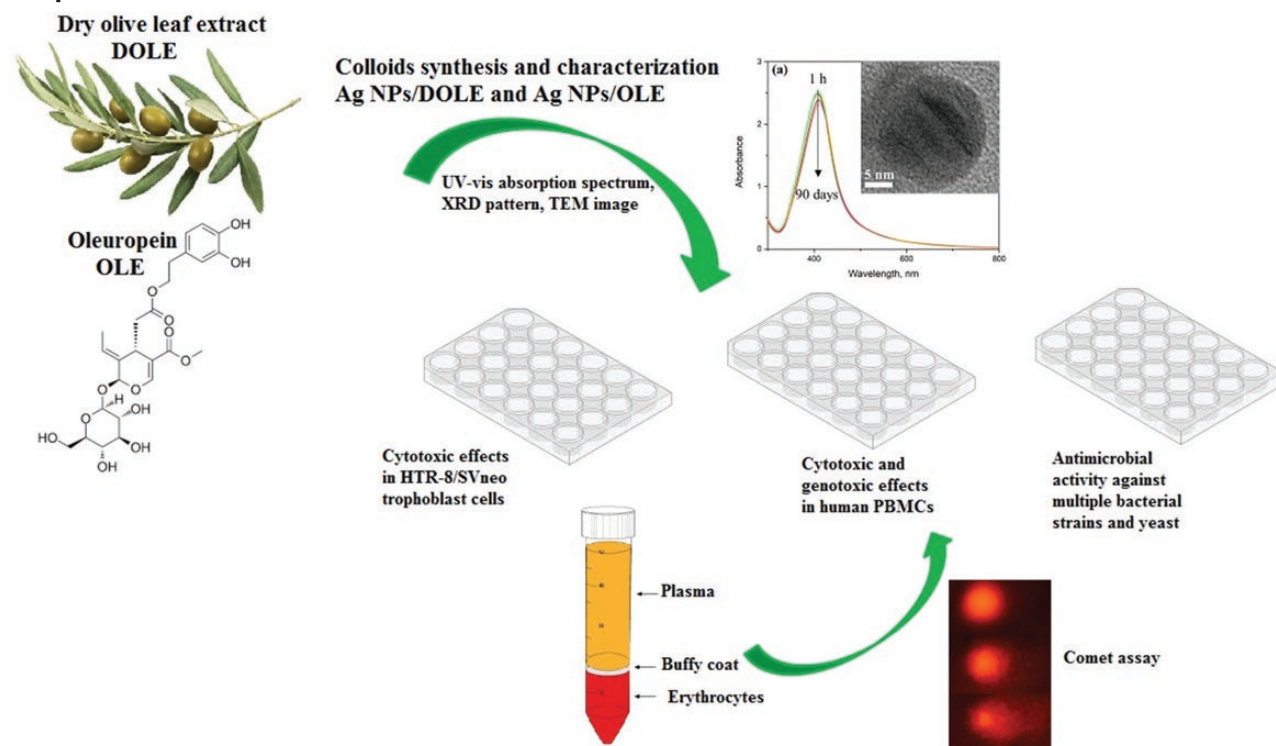
⁴Department of Microbiology and Immunology, Faculty of Pharmacy, University of Belgrade, Belgrade, Serbia

*Corresponding author. Department for Biology of Reproduction, Institute for the Application of Nuclear Energy-INEP, University of Belgrade, Banatska 31b street, 11000 Belgrade, Serbia. E-mail: andrea.pirkovic@inep.bg.ac.rs

Abstract

Dry olive leaf extract (DOLE) and its active component oleuropein (OLE) were applied as reducing and stabilizing agents to prepare colloidal 20–25 nm silver nanoparticles (Ag NPs). The Ag NPs were characterized using transmission electron microscopy, X-ray diffraction analysis, and absorption spectroscopy. The cytotoxic actions of coated Ag NPs, and their inorganic and organic components, were examined against trophoblast cells and human peripheral blood lymphocytes (PBLs), Gram-positive, Gram-negative bacteria, and yeast. The genotoxic potential was evaluated in PBLs *in vitro* with the comet assay. Ag/DOLE and Ag/OLE induced cytotoxic effects in both types of cells after 24 h exposure when silver concentrations were 0.025–0.2 mM. However, the most pronounced cytotoxicity exhibits Ag/OLE. Both colloids also caused reduced ROS production in both cell types at 0.1 mM and 0.2 mM, while bare Ag NPs did not alter ROS levels at any of the conditions. Functionalized Ag/DOLE and Ag/OLE did not show genotoxic effects in PBLs, while bare AgNPs increased DNA damage significantly only at 0.2 mM. Regarding the antimicrobial effects, the Ag/OLE had MIC values for all evaluated microorganisms from 0.0625 to less than 0.0312 mM. Also, the antimicrobial effect of Ag/DOLE was significantly higher on Gram-negative bacteria and yeast than on Gram-positive bacteria. Obtained results indicate that Ag/OLE induced the most pronounced biological effects, beneficial for its application as an antimicrobial agent, but with potential risks from exposure to high concentrations that could induce cytotoxicity in healthy human cells.

Graphical Abstract



Keywords: silver nanoparticles; cytotoxicity; olive leaf extract; oleuropein; antimicrobial effects

Introduction

One of the widely used nano-based products in biomedical applications is silver nanoparticles (Ag NPs) due to their unique characteristics. Therefore, Ag NPs are one of the most in-demand types of NPs due to their increasing use as novel antimicrobial agents, drug-delivery formulations, detection and diagnosis platforms, and coatings of medical devices. However, the current medical use of Ag NPs is hampered by their non-specific action because they display cytotoxicity to microbial and human cells at high concentrations or when agglomerated in cell nuclei causing intracellular oxidative stress and DNA damage [1,2]. Ag nanoparticles' toxicity depends on the concentration, size, shape, and functional groups present on the surface [1]. Thus, the functionalization of particle surfaces directly influences their toxicity and bioavailability. Recent studies indicated that plant phytochemicals (polyphenols, flavonoids, polysaccharides), in parallel, act as reducing and capping agents during the biogenic synthesis of Ag NPs, providing long-term stability of colloidal solutions [3,4]. By attaching appropriate organic groups to NPs, it is possible to increase their biocompatibility and modulate cellular internalization, prevent nanoparticle agglomeration, decrease their toxicity, and increase stability that is critical for biomedical applications. Recent studies indicated that the toxicity induced by Ag NPs prepared by the green synthetic route is lower compared to the Ag NPs obtained by colloidal chemical methods [5]. Thus, herbal-based Ag NPs are a potential solution for the next generation of nanomedicines with reduced toxicity and side effects on healthy cells.

The olive plant *Olea europaea* L. has been the focus of interest in medicine since ancient times [6]. Dry olive leaf extract (DOLE) from olive leaves is a rich source of phenolic and flavonoid compounds known as reducing agents for

nanoparticle synthesis [7,8]. DOLE is an ideal candidate for the biogenic production of Ag NPs due to its chemical composition and diverse biological and pharmacological activities, such as antimicrobial, antioxidant, antigenotoxic, and anti-inflammatory [9–16]. The most valuable active component in olive leaf extracts is oleuropein (OLE), a compound with a specific molecular structure that is an ester of elenolic acid and dihydroxyphenyl ethanol [14]. Besides oleuropein, other main derivatives of DOLE are hydroxytyrosol, tyrosol, *p*-coumaric acid, caffeic acid, vanillic acid, vanillin, luteolin, diosmetin, rutin, apigenin-7-glucoside, and luteolin-7-glucoside [14]. In a recent study, De Matteis *et al.* [7] showed that the Ag NPs prepared using the olive leaf extracts from two different olive varieties lead to the creation of NPs with diverse shapes, sizes, and different abilities to inhibit cancer cells growth, most likely due to differences in phytochemical content.

Oleuropein has been the subject of numerous scientific investigations due to its nutritional value and antioxidant, anti-inflammatory, and anti-cancer activities when used in nano-formulations [17–19]. Also, OLE can reduce Ag⁺ to Ag⁰ because of its electron-donating ability. Therefore, we prepared Ag NPs using DOLE and OLE to evaluate differences in physicochemical properties, cytotoxicity, effects on the production of reactive oxygen species (ROS), and genotoxicity between Ag NPs when OLE is solely present on their surfaces and when whole DOLE extract is present. So far, parallel investigation of Ag NPs functionalized with DOLE and by its main component OLE has never been conducted. Knowing that diverse outcomes with Ag NPs can be observed in different cell types, the studies of effects that they exhibit in particular cell types may provide a better understanding of their influence on safety and health.

Recent studies showed that Ag NPs have the ability to migrate across biological barriers and penetrate the cells in the human body via various exposure routes, thus accumulating in vital organs [20]. The potentially dangerous impacts of Ag NPs should be, in particular, evaluated in vulnerable states such as pregnancy, as toxicological consequences might be aggravated in enhanced susceptibility. Indeed, in recent studies, exposure to Ag NPs during pregnancy was found to affect both the placenta and the fetus in animals [21,22]. Due to the rising production and applications of silver nanoparticles and their increasing occurrence in the environment, leading to direct human exposure, there is an urgent need to enhance the understanding of the toxicity of Ag NPs on reproductive cells to achieve the design of nanomaterials with enhanced safety. HTR-8/SVneo cell line, originating from the first trimester of pregnancy placental explants, is an appropriate *in vitro* model for the preliminary testing of the toxicity of compounds transported to the placenta from the bloodstream [23]. The potential of Ag NPs functionalized with DOLE and OLE in human trophoblast cells has not been explored yet. Also, the effect of Ag NPs functionalized with DOLE and OLE on human peripheral blood lymphocytes (PBLs) will be evaluated for DNA damage, cell viability, and for the generation of ROS. Peripheral blood lymphocytes are sensitive to changes in systemic circulation and, because of that, are considered to be suitable for hemocompatibility testing of nanomaterials [24].

In the present study, we optimized synthetic parameters for preparing stable colloidal Ag NPs taking advantage of the dual function of DOLE as a reducing and capping agent. Besides, for comparison reasons, Ag NPs were prepared using solely OLE, whose concentration exactly matched its content in DOLE (20 wt.-%). The variation of synthetic parameters (concentration, pH, and temperature) led to optimized experimental conditions to achieve a one-pot synthesis of stable silver colloids (a couple of months). The synthesized colloidal Ag NPs functionalized with DOLE or OLE were thoroughly characterized using UV–Vis absorption spectroscopy, transmission electron microscopy (TEM), and X-ray diffraction (XRD) analyses.

The interaction of Ag NPs with human trophoblast cells and PBLs was investigated by evaluating their ability to induce cytotoxicity, increase ROS production and elevate DNA damage. This study aimed to test whether the functionalization of Ag NPs with DOLE or OLE significantly alters their biological effects and safety. Antimicrobial action of free-standing hybrid particles (Ag/DOLE and Ag/OLE) and their components (DOLE, OLE, and bare Ag NPs) was also estimated to determine the biocidal potential of these nanomaterials on representative strains of Gram-negative, Gram-positive bacteria, and yeast used in common applications in antimicrobial assays of antibiotics. The obtained results would provide a valuable contribution to the safety of Ag NPs and promote the application of the safe-by-design concept in the development of new antiseptics and Ag NPs-based formulations for human use.

Materials and methods

Synthesis and characterization of silver nanoparticles

The chemicals used in this study were all of the highest purity available and were used without further purification (J.T.

Baker, Centrohem). The solvent was Milli-Q deionized water (resistivity 18.2 M Ω cm⁻¹).

Commercially available DOLE (EFLA® 943, Frutarom Switzerland Ltd., Wadenswil, Switzerland) was manufactured using an ethanol extraction procedure (80% m/m), followed by filtration and standardization to 16–24% of oleuropein. The OLE is a commercial product purchased from *Extrasynthese, Genay, France* (CAS Number. 32619-42-4). The synthetic procedure for the preparation of stable colloidal Ag NPs was optimized by varying experimental parameters ($7 \leq \text{pH} \leq 11$, $0.002 \leq \text{concentration of extract} \leq 0.03$ (wt.-%), and $20 \leq \text{temperature} \leq 95^\circ\text{C}$), while the concentration of Ag⁺ ions was kept constant (0.2 mM). Briefly, the mixtures that consist of Ag⁺ ions and DOLE with chosen concentration, at chosen pH and temperature, were vigorously stirred for three hours. The appearance of the yellow-brown color indicated the formation of Ag NPs in the solution. The Ag colloids, stable for 6 months under ambient conditions, were obtained for the following synthetic parameters: 0.003 wt.-% DOLE, pH = 9, and $T = 60^\circ\text{C}$. For toxicity evaluation, colloids were prepared in phosphate buffer saline (PBS) solution (Fisher Scientific, Pittsburgh, PA), and their concentration was higher (1 mM), but the ratio between inorganic and organic components of hybrid nanoparticles was kept constant. Unmodified, bare Ag NPs were prepared using a strong reducing agent, NaBH₄, as described in our previous work [25].

The absorption spectra of Ag NPs colloidal solution were measured at room temperature using Thermo Scientific Evolution 600 UV–Vis spectrophotometer (Waltham, Massachusetts, USA). TEM was performed using a JEOL JEM-2100 LaB₆ instrument (Peabody, USA) operated at 200 kV coupled with a Gatan Orius CCD camera at 2 \times binning. The X-ray diffraction (XRD) patterns were recorded using a Rigaku Smart Lab instrument (Tokyo, Japan) under the Cu K α 1,2 radiation. Diffraction data were collected in a 2θ range from 10° to 90° , counting 0.7°/min in 0.01° steps. Dried silver colloids for XRD measurements were prepared using a spray drier (BÜCHI Mini Spray Dryer B-290 (Uster, Switzerland), inlet temperature 160°C , outlet temperature 85°C).

Isolation of lymphocytes

The peripheral blood samples were collected from three healthy participants (two female and one male, aged 20–25 years) that declared no use of alcohol, cigarettes, drugs, dietary supplements, or receiving any medical therapy in the month before and during this study. The Ethics Committee of the Faculty of Pharmacy, University of Belgrade, Serbia approved the study protocols (permit No. 1103/2). The research was performed following the Helsinki Declaration guidelines. Whole blood samples (5 ml) were drawn from a cubital vein and collected in lithium heparin vacutainers (Vacuette, Greiner Bio-One, Kremsmuenster, Austria), and further used for peripheral blood lymphocyte isolation. Blood, diluted with RPMI 1640 (Gibco, Waltham, MA, USA), was carefully poured on the top of the Ficoll–Paque medium (Sigma Aldrich, St. Louis, MO) without mixing two layers, and samples were centrifugated at $500 \times g$ for 15 min. After centrifugation, the buffy coat with cells above Ficoll–Paque was collected by Pasteur pipette and transferred into tubes. The samples were then washed in RPMI medium and centrifugated at $300 \times g$ for 10 min; this procedure was repeated twice. Finally, the pellet with cells was suspended in 1 mL of RPMI.

Cell culture and treatments

The HTR-8/SVneo trophoblast cell line and isolated PBLs were used to evaluate the effects of the DOLE, OLE, Ag/DOLE, Ag/OLE, and bare Ag NPs. PBLs were used immediately after isolation. Suspended lymphocytes in a complete RPMI medium were seeded in 96-well plates at a density of 3×10^5 cells/well. Treatments were added, immediately after seeding, in a final volume of 100 μ L per well. The HTR-8/SVneo cell line, originating from the first-trimester human placenta explant cultures immortalized with the SV40LT antigen, was kindly provided by Dr. Charles H. Graham, Queen's, Kingston, Canada. Cells were kept in 25 cm² tissue culture flasks in a humidified incubator at 37°C, with 5% CO₂. They were grown in a complete medium containing RPMI 1640 (Gibco, Waltham, MA, USA), 10% fetal calf serum (Gibco, Waltham, MA, USA), and 1% antibiotic–antimycotic solution (Capricorn Scientific GmbH, Ebsdorfergrund Germany). After reaching 70% confluence, the cells were trypsinized (0.25% trypsin-EDTA solution, Institute for Virology, Vaccines, and Serum 'Torlak', Belgrade, Serbia), seeded in 96-well plates (1.5×10^4 cells/well) and were let to attach to wells for 24 h at 37°C, 5% CO₂ before the treatment. The medium was exchanged after 24 h, and treatments were added in a total volume of 100 μ L/well. After the incubation with the treatments or solvent (control) at 37°C for 24 h, an MTT assay and H2DCFDA assay were performed.

Cytotoxicity evaluation (MTT assay)

Following the treatments, the medium was exchanged and fresh medium with MTT reagent (thiazolyl blue tetrazolium bromide, 1 mg/ml, Sigma Aldrich, St. Louis, MO, USA) was added (10 μ L per each well), and the cells were left for 2 h in the dark at 37°C for the reaction to occur. Further, purple formazan crystals were dissolved with sodium dodecyl sulfate (10% SDS in 0.01 M HCl, Sigma Aldrich, St. Louis, MO, USA). The absorbance was measured at 570 nm on a microplate reader (BioTek ELx800, VT, USA) after the complete solubilization of the crystals. Three independent experiments were performed in triplicates, $n = 3$.

H2DCFDA assay (2',7'-dichlorofluorescein diacetate)

After the 24 h treatments, media were removed and cells were rinsed with PBS. Next, H2DCFDA assay was performed in line with the manufacturer's instructions. Using PBS as the diluent, 5 μ M of the cell-permeable oxidation-sensitive probe, H2DCFDA (Merck Millipore, 2',7'-Dichlorofluorescein Diacetate—CAS 4091-99-0—Calbiochem) was added to the cells and left for 45 min in the dark. Next, the conversion of non-fluorescent H2DCFDA to the highly fluorescent 2',7'-dichlorofluorescein (DCF), which reflects the generation of intracellular ROS level in cells, was determined by measuring the fluorescence on a fluorescent plate reader (Wallac 1420 multilabel counter Victor 3V) at excitation and emission wavelengths of 485 and 535 nm, respectively. Data were expressed as normalized fluorescence intensity values, and plotted in relation to control. Three independent experiments were performed in triplicates, $n = 3$.

Comet assay

The cell number and viability of PBLs were assessed before treatments using the Trypan blue exclusion test to estimate the percentage of live/dead cells. The genotoxic potential

was evaluated by incubating PBLs with the different treatments for 1 h at 37°C and comparing observed effects to the controls treated only with the solvent (PBS). The level of DNA damage was evaluated by single cell gel electrophoresis (comet assay). Gel electrophoresis was carried out using prepared slides with PBLs, as described elsewhere [26] and following the MIRCA guidelines on comet assay [27]. Briefly, the cells on slides were lysed in lysing solution (10 mM Tris, 2.5 M NaCl, 100 mM EDTA, 1% Triton \times 100, 10% dimethylsulfoxide, pH = 10 set with NaOH) overnight at 4°C. The following day, the slides were placed in pre-chilled electrophoresis buffer (10 M NaOH, 200 mM EDTA) for 30 min in the horizontal gel electrophoresis tank (CHU2 manufacturer, connected to a Power Supplier EPS 601), and electrophoresis was run at 25 V and 300 mA (1.2 V/cm) for 30 min. After electrophoresis, slides were washed three times with neutralizing buffer (0.4 M Tris base, pH 7.5 adjusted with HCl), with a final wash in distilled water. The slides were then stained with ethidium bromide (20 mg/ml), and levels of DNA damage were assessed by visual classification of 'comet-like' nucleoids into five classes depending on the degree of DNA damage, according to the method by Collins *et al.* [28]. The analysis was performed using a fluorescent microscope (Olympus BX 50, Olympus Optical Co., GmbH, Hamburg, Germany), equipped with an HBO mercury lamp (Zeiss; 50W, 516–560 nm). Each of the observed comets was given a value of 0, 1, 2, 3, or 4 (from undamaged, 0 to totally damaged, 4), and DNA damage was expressed as arbitrary units with the following equation for calculation of total comet score (TCS): (percentage of cells in class 1 \times 1) + (percentage of cells in class 2 \times 2) + (percentage of cells in class 3 \times 3) + (percentage of cells in class 4 \times 4). Two replicate slides were analyzed per each treatment, and the scoring was performed on 100 randomly selected comets per slide. Experiments were repeated three times. DNA damage was expressed as the TCS.

Antimicrobial activity

The antimicrobial activity of bare Ag/DOLE, Ag/OLE, Ag NPs, DOLE, and OLE was evaluated by the broth microdilution method (The European Committee on Antimicrobial Susceptibility Testing. Breakpoint tables for interpretation of MICs and zone diameters. Version 11.0, 2021.; EUCAST reading guide for broth microdilution Version 4.0., <http://www.eucast.org>.) against the Gram-positive bacteria (*Staphylococcus aureus* subsp. *aureus* Rosenbach (ATCC 6538), *Staphylococcus epidermidis* (ATCC 12228), and *Bacillus subtilis* subsp. *spizizenii* (ATCC 6633)), the Gram-negative bacteria (*Escherichia coli* (ATCC 25922), *Klebsiella pneumoniae* subsp. *pneumoniae* (NCIMB 8267), *Salmonella enterica* subsp. *enterica* serovar Abony (NCTC 6017), and *Pseudomonas aeruginosa* (ATCC 27853)), and one strain of the yeast *Candida albicans* (ATCC 24433); all strains were purchased from Kwik-Stick, Microbiologics, USA.

Fresh overnight cultures were used to prepare the suspensions of microorganisms. One colony of each strain was suspended in a saline solution to a density of 0.5 per McFarland standard (Bio-Merieux, France), corresponding to a 1.5×10^8 CFU/ml of microorganisms. Further, microorganisms were diluted either in fresh Mueller–Hinton broth (MHB, Lab M Limited, UK) for bacteria or Sabouraud-dextrose broth (SB, Lab M Limited, UK) for *C. albicans*.

Serial dilutions of the treatment in MHB and SB were prepared, and 100 μl of each concentration was placed in triplicate in 96-well microtiter plates and inoculated with 100 μl of microorganisms. Final sample concentrations in the microtiter plate were in the range of 0.0312–0.5 mM, and the final concentration of microorganisms was 5×10^5 CFU/ml. Also, positive growth control (only microorganisms in medium) and negative control (only medium with samples) experiments were performed in triplicate. The plates were incubated in aerobic conditions at 35°C for 20 h, and the minimal inhibitory concentration (MIC) of each sample was determined as the lowest concentration of the treatment that inhibits the growth of microorganisms, that is, absence of turbidity or visible growth of microorganisms; tests were repeated three times. The MICs of referent antibiotics (ampicillin and nystatin) were determined in parallel experiments.

Statistical analysis

The data were analyzed using the ANOVA one-way analysis of variance with the Tukey posthoc test ($\alpha = 0.05$). The values were expressed as mean \pm standard error, and the differences were considered statistically significant at $P < 0.05$. GraphPad Prism 6.0 (GraphPad Software, Inc., USA) was used for statistical analyses.

Results and discussion

Optimization of synthetic parameters and characterization of Ag NPs

Dried olive leaf extract and its main component, oleuropein, were used to synthesize functionalized Ag NPs. The position and shape of the surface plasmon resonance band indicate the size distribution of silver particles in a colloidal solution

[29,30]. So, the absorption spectra of synthesized silver colloids were used to estimate optimal parameters for the synthetic procedure. In these experiments, the concentration of Ag^+ ions was kept constant (2.0×10^{-4} M), while the pH, concentration of the DOLE, and temperature were varied. Also, the stability of silver colloids, synthesized with DOLE, was followed up to an aging period of 3 months.

First, we studied the influence of pH on the formation of Ag NPs to determine a suitable acidity range. In Fig. 1a(i), we presented the absorption spectra at pH 7, 9, and 11, measured 24 h after the initiation of the reaction, while the concentration of DOLE was 0.003 wt.-% and the temperature was 60°C. At pH = 7, hydroxyl groups of OLE are protonated ($\text{pK}_a = 9.5$), which is the reason for the absence of the formation of metallic silver [31]. On the contrary, in alkaline media (pH = 9 and 11), the appearance of a distinct surface plasmon resonance band at ~ 400 nm indicates the formation of Ag NPs. However, at pH = 11, the absorption spectrum of silver colloid has a tail in the near-infrared spectral region due to the formation of larger/agglomerated Ag NPs. On the other side, at pH 9, when the reducing ability of polyphenols is moderate, the number of initially formed nuclei is proper and their consequent growth results in the formation of non-agglomerated silver nanoparticles indicated by the narrow surface plasmon resonance band [32]. So, we can conclude that the optimal pH value for the biosynthesis of silver colloids is 9. A similar acidity was found suitable for the Ag NPs preparation using polyphenols from the different biological extracts [3,33].

Fig. 1(A)(ii) shows the influence of extract concentration on the absorption spectra of Ag colloids; pH (9.0) and temperature (60°C) were kept constant. Except for the highest concentration of DOLE (0.03 wt.-%), the surface plasmon

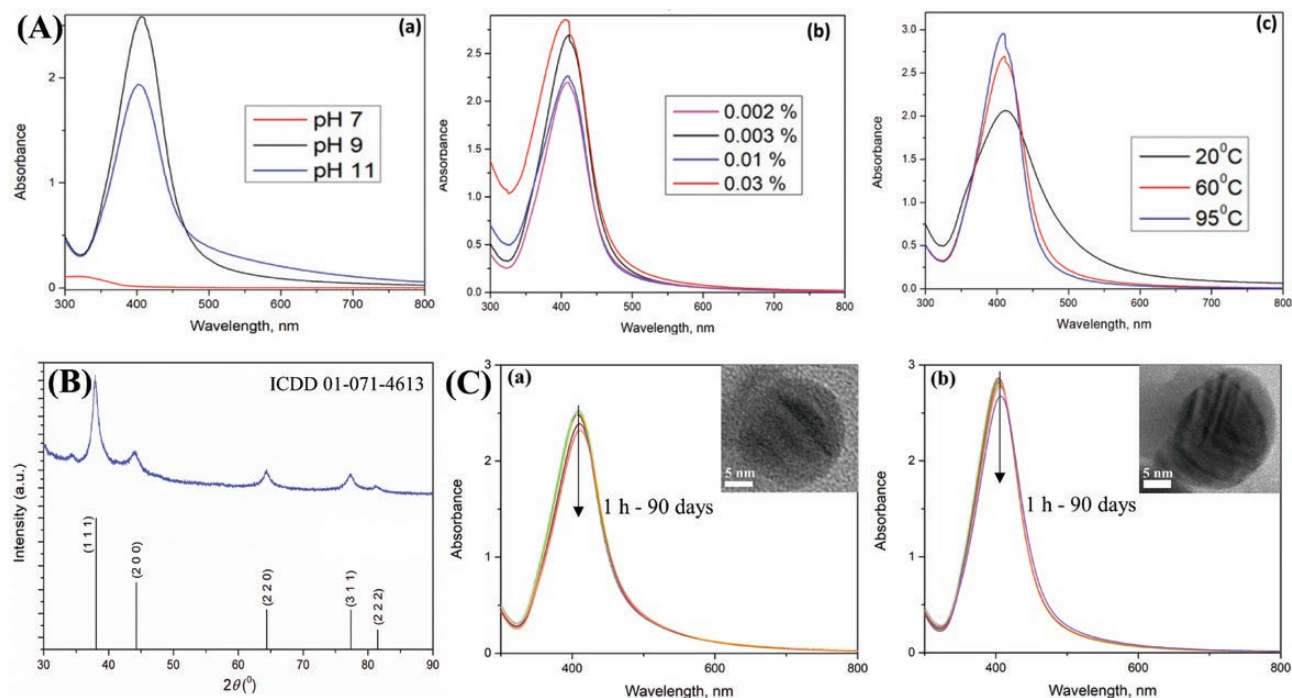


Figure 1. (A) Absorption spectra of Ag NPs colloid solution as a function of (a) concentration of olive leaf extract, (b) pH, and (c) temperature. Experimental conditions: (a) 2×10^{-4} M Ag^+ , pH = 9, $T = 60^\circ\text{C}$, (b) 2×10^{-4} M Ag^+ , 0.003 wt. % of DOLE, $T = 60^\circ\text{C}$, and (c) 2×10^{-4} M Ag^+ , 0.003 wt. % of DOLE, pH = 9. All spectra were measured 24 h after the initiation of the reaction. (B) The XRD pattern of Ag/DOLE powder sample. (C) Absorption spectra of (a) Ag/DOLE and (b) Ag/OLE colloids as a function of aging time. Typical TEM images of Ag NPs after 3 months of aging are shown in insets.

resonance band peaking at 411 nm, and the spectra have the same shape. However, when the DOLE concentration is low (0.002 wt.-%), the concentration of deprotonated hydroxyl groups is insufficient to reduce all Ag⁺ ions. Since the DOLE concentration must be below 0.03 wt.-%, the 0.003 wt.-% of DOLE is considered optimal for the Ag NPs preparation.

Finally, we analyze the influence of temperature (20°C, 60°C, and 95°C) on the formation of silver colloids (Fig. 1a(iii)); other synthetic parameters were kept constant (0.003 wt.-% DOLE, pH = 9.0). The spectra were measured 3 h after the initiation of the reaction. At the lowest investigated temperature (20°C), the growth of Ag NPs is slow, and the absorption band is broad. At higher temperatures (60°C and 95°C), the intensity of absorption maxima increases, followed by a narrowing of the surface plasmon resonance band. Since almost identical optical behavior Ag NPs has when prepared at 60°C and 95°C, the lower temperature is a more suitable option for their synthesis. To conclude, the following set of experimental conditions is used further in this study to synthesize functionalized Ag NPs with DOLE (0.003 wt.-% DOLE, pH = 9, T = 95°C). The synthesis of OLE, the main component of DOLE, was carried out under identical experimental conditions; the only difference was that the applied concentration of OLE corresponds to its content in DOLE (20 wt.-%).

The XRD pattern of Ag/DOLE is shown in Fig. 1b, while we omitted for clarity reasons the identical XRD pattern of Ag NPs/OLE. The diffraction peaks at 37.9°, 44.1°, 64.4°, 77.3°, and 81.3° correspond to the (111), (200), (220), (311), and (222) crystal planes of face-centered-cubic silver (COD 01-071-4613), respectively. Scherrer's equation was applied to estimate the average crystallite size in Ag NPs (~4 nm).

Representative TEM images of capped Ag NPs with DOLE and OLE are shown in the insets of Fig. 1c. Both colloidal solutions consist of nearly spherical crystalline Ag particles whose size ranges from 20 to 25 nm. Internal grain structure, frequently observed for metal nanoparticles, is evident on TEM images, with each nanoparticle typically containing several subdomains.

The long-term stability of Ag colloids is a prerequisite for their biomedical application. So, the shelf-life stability of Ag colloids, prepared by optimized synthetic conditions (0.003 wt.-% DOLE or 0.0006 wt.-% OLE, pH = 9.0, T = 60°C), was followed as a function of aging time using UV-Vis spectroscopy (see Fig. 1c). It should be noticed that after 3 months of aging in both silver colloids (Ag/DOLE and Ag/OLE), only a slight decrease in absorption maxima (less than 10%) was observed without any change in spectral features. Knowing that the complete dissolution of bare Ag NPs, prepared by NaBH₄, occurs for a couple of days [34], enhanced stability of hybrid nanoparticles is a significant step forward in their safe use in biomedicine. While the formation of Ag NPs is induced by electron transfer reaction from deprotonated hydroxyl groups to Ag⁺ ions [3,4,35], their stability is a consequence of diminished oxygen access due to the presence of organic components on the surface and reducing environment that prevent oxidation, additionally provided by free ketone and aldehyde groups.

Cytotoxic evaluation of Ag/DOLE and Ag/OLE

The toxic action of Ag NPs rises with a decrease in organisms' complexity, from mammalian cells to viruses [36–38]. Earlier

studies of the toxicity of nanoparticles in various human cells revealed that they could display selective toxicity in particular cellular lines [39]. Among many human cell models available, PBLs are the most common platform for the evaluation of cytotoxic effects and genotoxicity of nanostructures. The sensitivity of cell lines to Ag NPs is different compared to primary cultures, and because of that, the use of PBLs is strongly recommended to be the first step to determining the cytotoxicity and genotoxic damage induced by nanomaterials [40,41].

The results, presented in Fig. 2a, indicate that exposure of PBLs to 24 h treatment with the Ag/DOLE and Ag/OLE (0.025–0.2 mM Ag NPs with proper contents of DOLE and OLE) leads to significant cytotoxic effects compared to the control sample, the sample only treated with solvent. On the other side, the exposure of PBLs to the bare Ag NPs, prepared by NaBH₄ and having the same range of concentrations, significantly altered cell viability only at the two highest concentrations (0.1 and 0.2 mM Ag NPs), while the observed reduction percentages of alive cells are small (77.4% and 81.9% viability, respectively). Also, the exposure of PBLs to the organic components of hybrid nanoparticles (DOLE and OLE) having corresponding concentrations did not significantly alter cell viability. So, the most pronounced cytotoxicity was induced by the exposure to the Ag/OLE, and consequently, the observed cytotoxicity reached a maximum at the highest concentrations (20.5% and 16.6% viability for 0.2 and 0.1 mM Ag NPs, respectively).

The alteration of morphology in normal cell and cell loss is observable in both PBLs treated for 24 h with Ag/DOLE and Ag/OLE (Fig. 3c and d). The Ag NPs treated cells are rounded, decreased in number, with nanoparticles present inside the cells and in the extracellular environment, in contrast to the untreated (control) cells which look healthy with no apoptotic or necrotic cells. Apoptosis and decreased proliferation of cells are common responses to *in vivo* and *in vitro* treatment with Ag NPs. The extent of cytotoxicity depends on the size, concentration, agglomeration, and functionalization of Ag NPs, silver ions release, and cell types used [42]. Several mechanisms could be responsible for nanoparticle-mediated *in vitro* toxicity. Besides direct cytotoxicity, mediated by apoptosis and/or necrosis, indirect mechanisms that include changes in the production level of ROS, lipid peroxidation, and genotoxic effects can also induce cell death [43]. In a recent study, Malysheva *et al.* [44], emphasized that the toxic effect of Ag NPs in human lymphocytes primarily depends on their uptake (amount), while the size and property of surface coating are of less importance. So, the cytotoxicity threshold is strongly influenced by the intracellular mass of silver per cell. The different cellular uptake of functionalized Ag NPs compared to bare ones is the most likely the reason for the differences in toxic behavior observed in our study. The cellular uptake of Ag/DOLE and Ag/OLE could be higher than the bare ones due to the coordination of organic molecules on the nanoparticle's surface, resulting in increased intracellular silver concentration and toxicity. However, this remains an open question, subject to further investigation.

Ruiz-Ruiz *et al.* [40], showed that Ag NPs, in the same concentration range used in this study, induced pronounced growth inhibition in pathogenic bacteria and tumor cells while producing only moderate cytotoxicity and DNA damage in human primary lymphocytes. The factors such as the physicochemical characteristics could strongly influence the

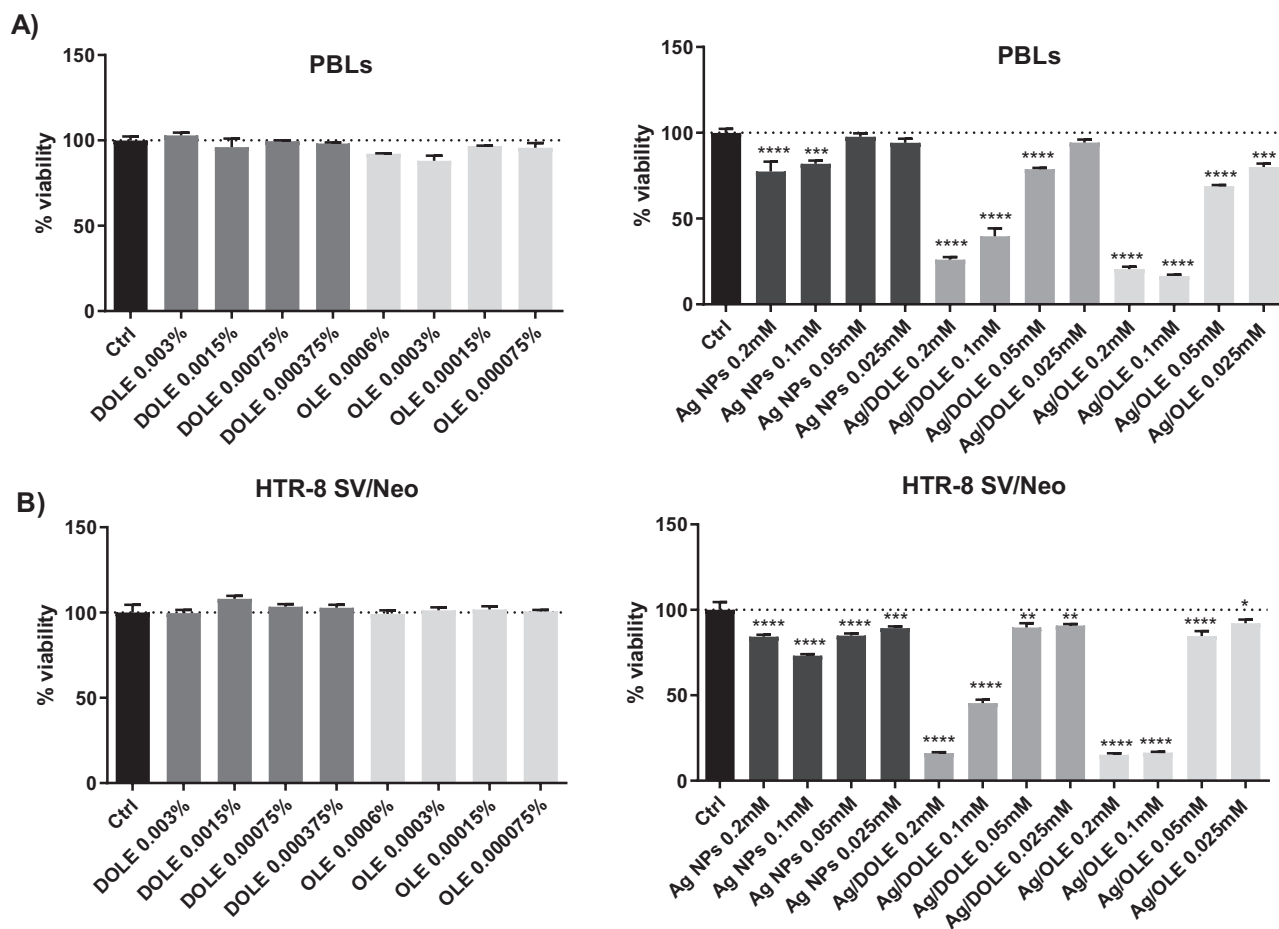


Figure 2. Cytotoxic effect of DOLE, OLE, Ag/DOLE, Ag/OLE, and bare Ag NPs in (A) human PBLs and (B) HTR-8/SVneo cells. The data are expressed as mean \pm SEM. * $P < 0.05$, ** $P < 0.01$, *** $P < 0.001$, **** $P < 0.0001$ versus control.

biological response of cells to different Ag NPs formulations, but the differential cytotoxicity also depends on the used cell type. Thus, we used identical formulations of Ag NPs and evaluated their cytotoxicity to HTR-8/SVneo trophoblast cells. These cells are used as *in vitro* models for the primary cytotrophoblast of first-trimester pregnancy since they show similar features in various functional assays [45–47]. Although it is well-known that Ag NPs can easily penetrate the placental barrier, and there are indices of developmental toxicity from animal studies [22], the literature data concerning the activity of silver nanoparticles at the human fetomaternal interface, especially trophoblast cells, are almost non-existent. The transport mechanism of Ag NPs in the placenta is currently not fully understood, but there are indications that endocytosis could be a pathway that mediates the placental transfer of NPs in trophoblasts [22].

The HTR-8/SVneo trophoblast cells, exposed 24 h to functionalized and bare Ag NPs, showed a significant reduction of cell viability for all silver concentrations, lower and higher (Fig. 2b). The treatment with Ag/OLE induced the most pronounced cytotoxicity, indicated by a significant decrease in cell viability (15.2% and 16.4% for 0.2 and 0.1 mM Ag NPs, respectively). However, the cytotoxic effect is concentration-dependent upon cell treatment with Ag/DOLE and Ag/OLE while bare Ag NPs showed similar effects at all concentrations. This observation supports the morphological characterization of cells, where the treatment

with smaller concentrations of silver (less than 0.2 mM) produced fewer changes, such as cytoplasmic vacuolization and alteration of cell morphology from normal to round-shaped cells. Alterations in HTR-8/SVneo trophoblast cell morphology after 24 h treatments with the highest concentration of functionalized and bare Ag NPs (0.2 mM) are shown in Fig. 3. The exposure to bare Ag NPs slightly reduces the number of normal cells, while agglomerated nanoparticles are noticeable throughout the sample (Fig. 3f). On the contrary, almost complete loss of normal cells and many round-shaped cells can be observed after the treatment with Ag/OLE (Fig. 3h) compared to the control with healthy-looking cells (Fig. 3e). The cell incubation with the Ag/DOLE induced similar toxic effects as Ag/OLE since normal cells are scarcely present following the treatment (Fig. 3g).

Recently, Costa *et al.* [48], demonstrated a lack of cytotoxicity after 24 h incubation of HTR-8/SVneo and BeWo trophoblast cells with biogenic Ag NPs, synthesized by *F. oxysporum*, with an average size of 69 nm. These authors explained the low toxicity of Ag NPs by their large size. So, significant concentration-dependent cytotoxicity in HTR-8/SVneo cells, observed in this study, using the same concentration of smaller size Ag NPs (25 nm) is in line with the assumption that smaller nanoparticles have increased uptake in cells and display more pronounced cytotoxicity because of a larger surface area and the capacity to translocate across cell barriers [49]. The literature data on the proliferation and

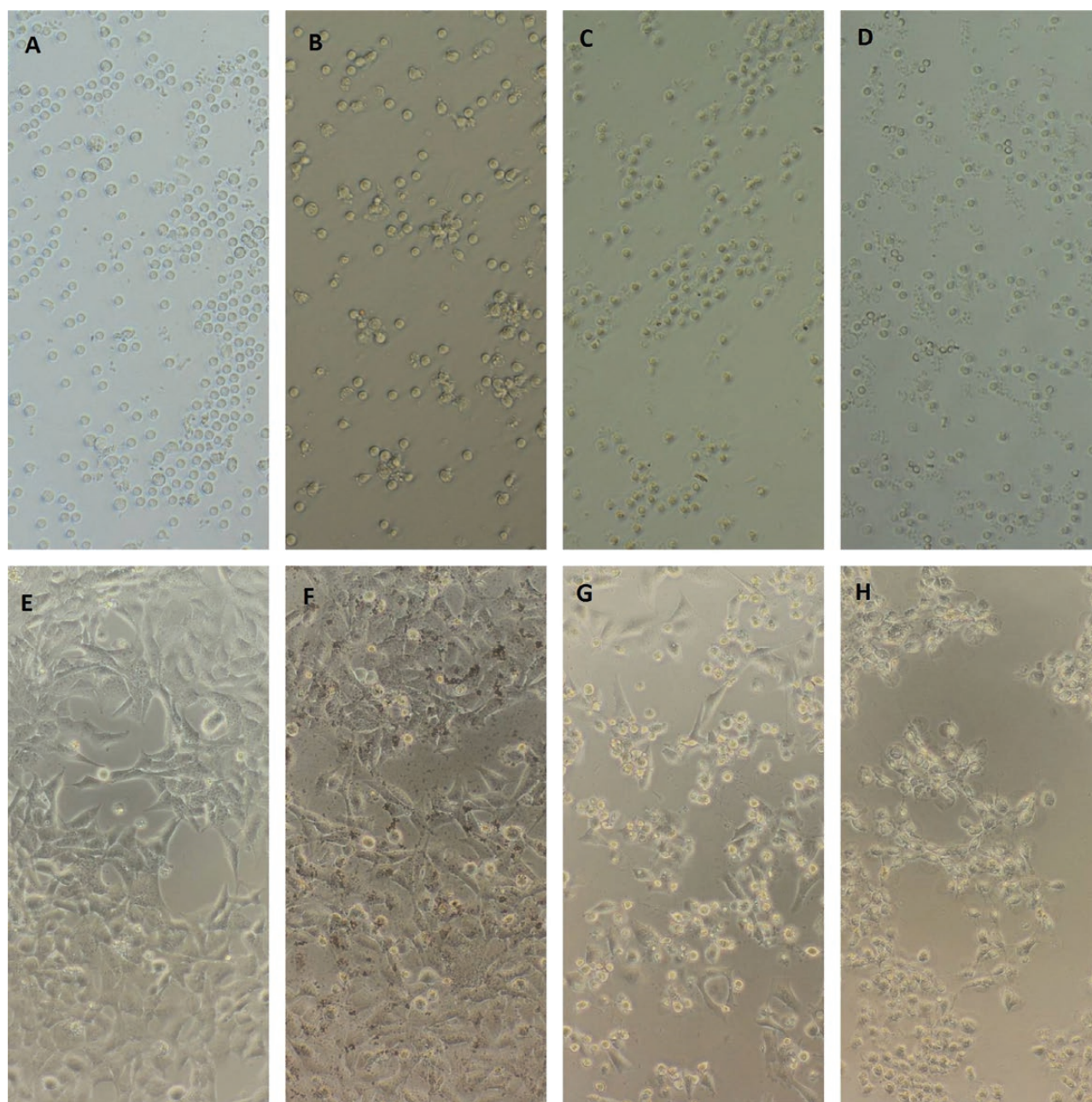


Figure 3. Morphological changes in PBLs (A–D) and HTR-8/SVneo cells (E–H) after 24 h treatments with (a and e) untreated (control) (B and F), Ag NPs (C and G), Ag/DOLE and (D and H) Ag/OLE. Concentration of silver colloids was kept constant (0.2 mM).

flow cytometry analysis of HeLa cells treated with Ag NPs indicate concentration-dependent cytotoxicity [50]. The higher concentrations of Ag NPs, used in this study and the concentration of Ag NPs synthesized by De Matteis *et al.* [7] are comparable. These authors reported a significant reduction in HeLa cell viability after the treatment of 48 h, which is in agreement with our results showing reduced viability of HTR-8/SVneo cells after 24 h exposure to Ag/DOLE and Ag/OLE.

Influence of Ag/DOLE and Ag/OLE on ROS production in cells

To further elucidate the toxic action of colloids, we analyzed the effects of 24 h incubation with bare AgNPs, Ag/

DOLE, and Ag/OLE on the ROS production in cells. Reactive oxygen species are produced as a result of cellular oxidative metabolism and their levels are known to influence cell survival, cell signaling, apoptosis [51]. The metallic NPs are known to produce ROS-mediated toxicity via Fenton-type reactions [51]. Previous research showed that surface coating of NPs and active sites on the NP surfaces have a direct impact on ROS production [52]. Silver nanoparticles (AgNPs) of 30 nm size were previously evaluated for ROS production in neuroblastoma SH-SY5Y cells and were shown to induce ROS production in a concentration-dependent and time-dependent manner [53]. In our research, the range of concentrations (0.025–0.2mM) was used to evaluate the impact of all three types of nanoparticles on ROS production in human lymphocytes and trophoblast cells. Following the

24 h incubation, the levels of ROS in lymphocytes (Fig. 4a) did not change in cells exposed to bare AgNPs, while levels of ROS in cells treated with Ag/DOLE and Ag/OLE showed a significant reduction of ROS production at concentrations 0.2 mM and 0.1 mM. Similar effect was observed in HTR-8 SV/Neo cells where bare AgNPs did not change ROS production in cells, while the highest concentrations of Ag/DOLE and Ag/OLE reduced ROS levels significantly (Fig. 4b). The most pronounced effect was observed in treatment with Ag/OLE where even the smaller concentrations (0.025 mM and 0.05 mM) produced a significant reduction of ROS. Since the decrease of ROS production, visualized by the reduced intensity of fluorescein generated from H2DCFDA follows the same pattern as the results of cytotoxicity evaluation, it could be concluded that the observed reduction of ROS was due to a smaller number of viable cells, and not from the antioxidant effect of colloids. This is further supported by the fact that DOLE and OLE extracts *per se* did not reduce ROS production in cells in same concentrations as those found in colloids.

Genotoxic properties of Ag/DOLE and Ag/OLE

We evaluated the genotoxic effects of functionalized and bare Ag NPs to get a deeper understanding of their action mechanisms. The genotoxic potentials of Ag/DOLE, Ag/OLE, and bare Ag NPs in PBLs, obtained *via* comet assay, are presented in Fig. 5. The investigated colloids of Ag/DOLE and Ag/OLE whose maximum concentrations were 0.2 mM, showed a slight increase of DNA damage but did

not exhibit a significant genotoxic effect after one-hour exposure compared to controls, treated only with solvent. However, bare Ag NPs showed a significant increase of DNA damage compared to controls at a concentration of 0.2 mM ($P < 0.05$) (Fig. 5). The representative images of comets exposed to colloids demonstrated the presence of fragmentation of DNA, while controls contained round nuclei without any damage (Fig. 5). At concentrations lower than 0.2 mM, none of the tested colloids showed genotoxic effects.

Taking into consideration previously published results [54–56] that indicate the genotoxicity of bare Ag NPs due to the break of DNA, mutations, and base oxidation, our results are in line with these findings. Previous research by Huk *et al.* [55] indicates that the impact of Ag NPs on the level of DNA damage is related to surface charge and surface coating. Furthermore, Lebedová *et al.* [57] found that the genotoxicity depends on Ag NPs size; for example, 50 nm in size particles are less genotoxic than 5 nm in size. Our results showed that 25 nm in size functionalized Ag NPs are not genotoxic to human PBLs after a one-hour exposure time. Butler *et al.* [56] emphasized that cellular uptake of Ag NPs crucially influences a genotoxic cell response and that particles, in the case of mammalian cells, are contained within intracellular vesicles but never within the nucleus. The same authors indicated that DNA damage by Ag NPs occurs upon exposure to the 10–20 nm-sized particles but not upon exposure to the 50–100 nm-sized particles at concentrations above 25 $\mu\text{g}/\text{ml}$, suggesting both size-dependent and concentration-dependent effects. We also observed concentration-dependent effects where

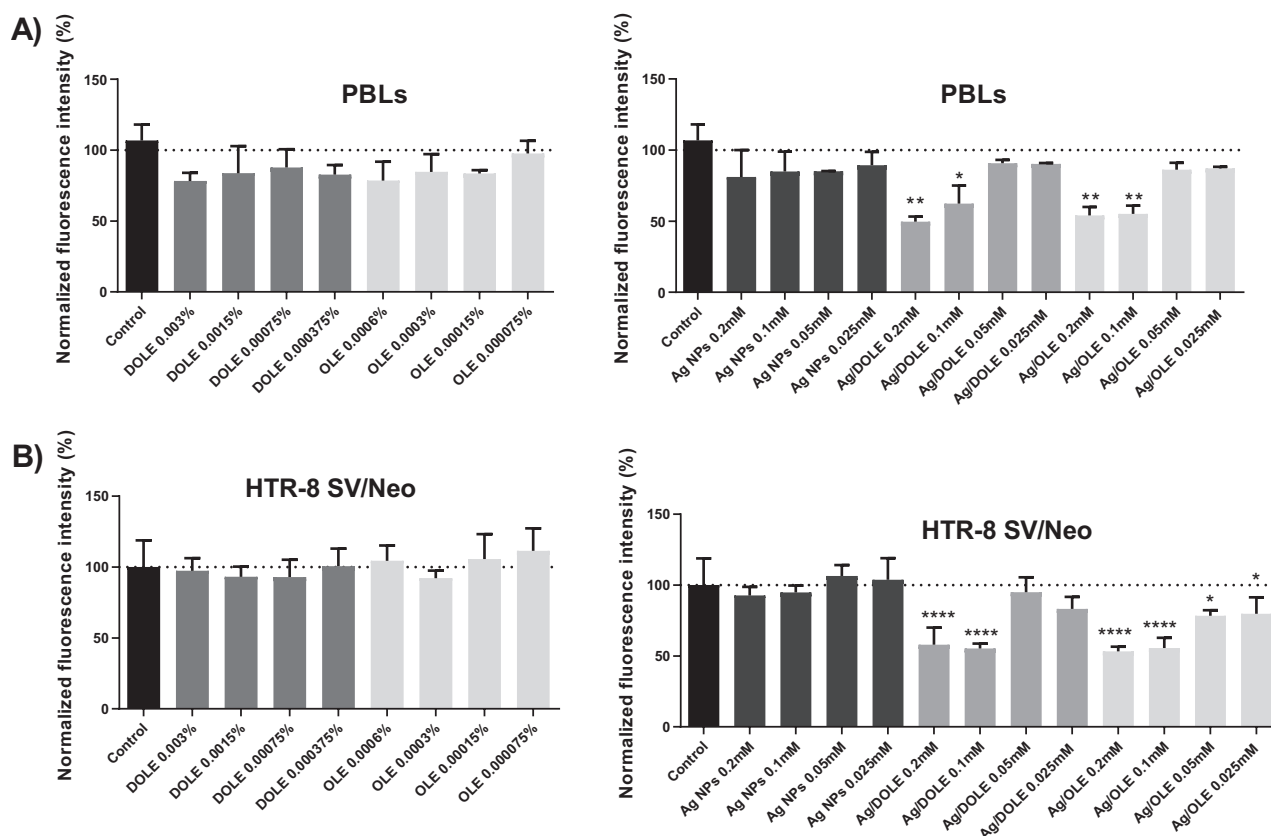


Figure 4. Modulation of ROS generation by DOLE, OLE, Ag/DOLE, Ag/OLE, and bare Ag NPs in (A) human PBLs and (B) HTR-8/SVneo cells. The data are expressed as mean \pm SEM. * $P < 0.05$, ** $P < 0.01$, *** $P < 0.001$, **** $P < 0.0001$ versus control.

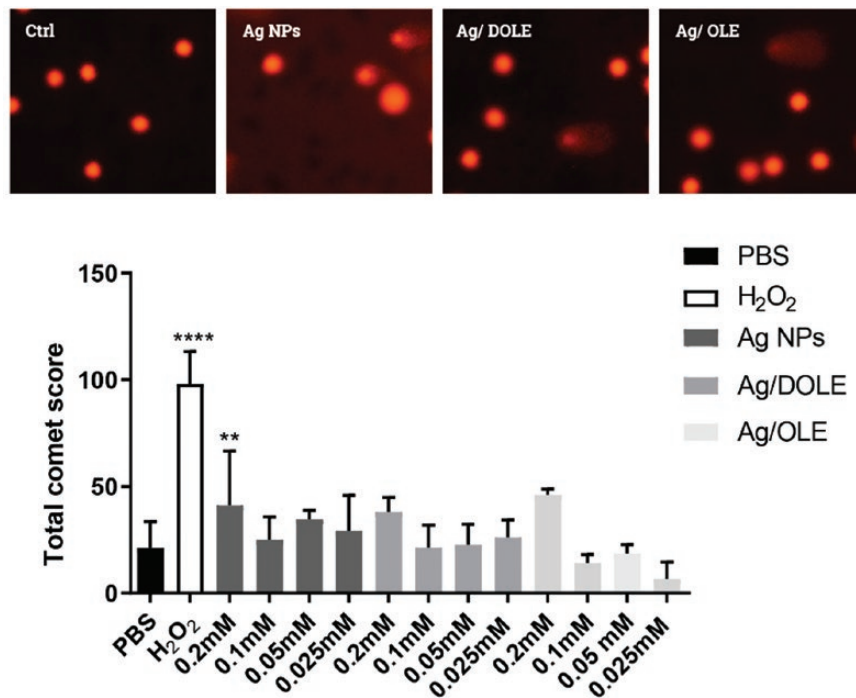


Figure 5. Lower panel: Genotoxic effect of Ag/DOLE, Ag/OLE, and bare Ag NPs in PBLs, obtained by comet assay, presented as TCS in bars. The data are expressed as mean \pm SEM. * $P < 0.05$, **** $P < 0.0001$. Upper panel: The representative comet assay images of PBLs stained with ethidium bromide, given for each treatment, Ag/DOLE, Ag/OLE, and bare Ag NPs.

concentrations less than 0.2 mM did not induce any DNA damage. Also, these authors proposed that released silver ions may be the primary source of genotoxicity in the DNA damage response since the Ag NPs were not in direct contact with nuclear DNA. So, in our study, the bare AgNPs showed significant genotoxicity probably as a result of a release of silver ions, while surface functionalization in Ag/DOLE and Ag/OLE could be reasons for the lack of Ag NPs genotoxicity observed in human PBLs, due to smaller release of silver. Also, it is worth mentioning that Joksic *et al.* [58]. have found that Ag NPs, different in size and concentrations, can produce diverse biological effects in human lymphocytes, varying from those exhibiting cells stasis without direct deteriorating effects on DNA, while others induced adverse effects on the cell membrane and produced cell death and double-strand breaks. DNA damage and instability are critical aspects of carcinogenesis, and malfunction of the DNA repair process can be associated with the initiation and progression of carcinogenesis. It is well-known that plant-derived bioactive compounds (phytochemicals) reduce the risks of cancer development by protecting DNA against damage, neutralizing carcinogens, or inducing DNA repair [59]. Our previous work also showed that DOLE decreased the number of DNA-damaged cells after H₂O₂ exposure [60]. It should be mentioned that the treatments with pure DOLE and OLE in the current study did not induce an increase in DNA damage compared to control (data not shown). The lack of genotoxicity of OLE *per se* in human lymphocytes *in vitro*, observed in this study, is consistent with a previous report by Zorić *et al.* [61]. To conclude, our results indicate that the attachment of DOLE and OLE on the surface Ag NP reduces their genotoxic potentials since the tested bare Ag NPs increased the numbers of DNA-damaged cells compared to controls after 1 h exposure. However, the limitation of this study is the incubation time, which might

reflect the short-term genotoxic effects but cannot provide conclusions about the consequences of prolonged exposure.

Antimicrobial activity of Ag NPs, Ag/DOLE, and Ag/OLE

The antimicrobial activities of Ag NPs, bare and coated with DOLE or OLE, are presented in Table 1. Bare Ag NPs display antimicrobial activity against all tested Gram-positive bacteria (*S. aureus*, *S. epidermidis*, and *E. faecalis*) and yeast *C. albicans* with MIC concentrations ranging from 0.25 to 0.50 mM. However, MICs for Gram-negative bacteria were not determined since the effect was the above-tested concentration of 0.50 mM. On the other side, Ag NPs coated with DOLE and OLE have significantly reduced MIC values compared to bare Ag NPs in all tested microorganisms except for *S. aureus* (2–16 times for Ag/DOLE and 8–16 times for Ag/OLE). The antimicrobial action of Ag/DOLE was significantly higher on *C. albicans* and Gram-negative bacteria except for *E. coli*, with MIC values ranging from 0.0625 mM to less than 0.0312 mM, compared to MIC values obtained for Gram-positive bacteria (0.125 mM). On the contrary, there is no difference in the antimicrobial activity of Ag/OLE on Gram-positive and Gram-negative bacteria since all MIC values ranged from 0.0625 mM to less than 0.0312 mM except for *S. aureus*. DOLE or OLE alone had no antimicrobial effect in all tested strains of microorganisms.

The precise mechanism of antimicrobial activity of Ag NPs, Ag/DOLE, and Ag/OLE has not been elucidated yet. The discrepancy in antibacterial effect between Gram-positive and Gram-negative bacteria could be a result of differences in the cell wall structures and their permeability. Gram-positive bacteria have a mainly peptidoglycan-built (N-acetylglucosamine and N-acetylmuramic acid, and a variety of amino acids) thick cell wall, compared to the Gram-negative bacteria, which have

Table 1. Antimicrobial ability of Ag NPs, Ag/DOLE, Ag/OLE, DOLE, and OLE

| Sample | Microorganism | | | | | | | |
|---------|------------------------------|-----------------------------------|--------------------------|-------------------------|------------------------------|----------------------------|-------------------------------|-------------------------|
| | <i>Staphylococcus aureus</i> | <i>Staphylococcus epidermidis</i> | <i>Bacillus subtilis</i> | <i>Escherichia coli</i> | <i>Klebsiella pneumoniae</i> | <i>Salmonella enterica</i> | <i>Pseudomonas aeruginosa</i> | <i>Candida albicans</i> |
| Ag NPs | 0.25 mM | 0.5 mM | 0.25 mM | >0.5 mM | >0.5 mM | >0.5 mM | >0.5 mM | 0.5 mM |
| Ag/DOLE | 0.125 mM | 0.125 mM | 0.125 mM | 0.125 mM | ≤0.0312 mM | ≤0.0312 mM | 0.0625 mM | ≤0.0312 mM |
| Ag/OLE | 0.125 mM | ≤0.0312 mM | ≤0.0312 mM | 0.0625 mM | 0.0625 mM | 0.0625 mM | 0.0625 mM | ≤0.0312 mM |
| DOLE | >0.5 mM | >0.5 mM | >0.5 mM | >0.5 mM | >0.5 mM | >0.5 mM | >0.5 mM | >0.5 mM |
| OLE | >0.5 mM | >0.5 mM | >0.5 mM | >0.5 mM | >0.5 mM | >0.5 mM | >0.5 mM | >0.5 mM |
| Blank | >0.5 mM | >0.5 mM | >0.5 mM | >0.5 mM | >0.5 mM | >0.5 mM | >0.5 mM | >0.5 mM |

a more complex structure with a thin peptidoglycan layer between the external and interior cell membrane. Additionally, the outer membrane in the Gram-negative bacteria is abundant with transmembrane porin proteins that actively participate in the transmembrane transport of molecules. The size of the pores and the position of the amino acids inside the channel influence the static properties of porins, and transport through them is dependent on the size, charge, and lipophilicity of the transported molecules [62]. As previously mentioned, Ag NPs have a non-specific microbicidal effect due to agglomeration in cell nuclei, DNA damage, and intracellular oxidative stress [2], but yet the precise mechanism behind their antimicrobial activity is not fully understood. The different biological response of Gram-positive and Gram-negative bacteria on Ag NPs is the most likely consequence of differences in their cell wall structures that cause different permeability of their cell walls [63,64]. The yeast *C. albicans* is a eukaryotic organism, and eukaryotic cells have a different structure of cell walls and plasma membranes compared to prokaryotic bacteria. The transport of *C. albicans* through the cell membrane is similar to other eukaryotic cells.

Since our results indicate that bare Ag NPs have lower antimicrobial activity compared to Ag/DOLE and Ag/OLE, we assume that the transport through cell walls (cell membranes) of Gram-positive and Gram-negative bacteria, and yeast is facilitated by the presence of organic molecules (DOLE and OLE) attached to the surface of Ag NPs. Considering the MIC values of bare Ag NPs and pure DOLE and OLE, it is clear that there is a synergy effect in antimicrobial action between the inorganic and organic constituents of hybrid nanoparticles. Additionally, we want to stress that the observed antimicrobial effect cannot be attributed to the cytotoxic properties of Ag/DOLE and Ag/OLE. We already mentioned that Ag/DOLE and Ag/OLE display the cytotoxic effect on PBLs and HTR-8/SVneo trophoblast cells for concentrations significantly higher compared to most MIC values. These findings agree with the study by Ruiz-Ruiz *et al.* [40], who reported that Ag NPs at the same concentrations used in this study have an inhibitory effect on the growth of malignant cells or bacteria and minimal cytotoxic effects on other cells like primary human lymphocytes.

Conclusion

For the first time in this study, the comparative biological effects of Ag NPs, synthesized using DOLE, and its main

component, OLE, in trophoblast cells and human PBLs were analyzed. Based on the obtained data, it can be concluded that functionalized Ag NPs with DOLE and OLE produce cytotoxic effects in both types of cells at concentrations of 0.2 and 0.1 mM. However, the more pronounced cytotoxicity is exhibited by Ag/OLE. Second, the results showed that bare AgNPs do not influence ROS levels in lymphocytes and trophoblast cells under described conditions, while reduced ROS production was exhibited in cells treated with Ag/DOLE and Ag/OLE, probably resulting from cytotoxic effects and a reduced number of live cells. In terms of genotoxicity, neither Ag/DOLE nor Ag/OLE showed genotoxic effects in human PBLs following the 1 h exposure, while exposure to bare Ag NPs increased the levels of DNA damage only at the highest concentration of 0.2 mM. Finally, both Ag/DOLE and Ag/OLE displayed antimicrobial activity, but Ag/OLE had more potency since MIC values, evaluated for Gram-positive bacteria, Gram-negative bacteria, and *C. albicans*, except for *S. aureus*, ranged from 0.0625 to less than 0.0312 mM. On the other side, the antimicrobial effect of Ag/DOLE was significantly higher on Gram-negative bacteria and *C. albicans* than on Gram-positive bacteria.

To briefly conclude, the obtained results indicate potential risks from exposure to high concentrations of Ag NPs in trophoblast cells, which can be of particular concern in the early stages of pregnancy. On the other hand, knowing that Ag/OLE induced remarkable antimicrobial effects, further studies are required to identify the safe concentrations that would lack cytotoxic effects on healthy human cells while maintaining the desirable biocidal effects against microorganisms.

Data Availability

The data underlying this article will be shared on reasonable request to the corresponding author.

Acknowledgments

We would like to express our gratitude to Professor S.P. Ahrenkiel, South Dakota School of Mines and Technology, USA for performing TEM measurements.

Conflict of Interest

The authors report no competing interests.

Funding

This research was funded by the Ministry of Education, Science and Technological Development, Republic of Serbia through a Grant Agreement with the University of Belgrade-Institute for the Application of Nuclear Energy-INEP, University of Belgrade-Faculty of Pharmacy and University of Belgrade-Vinča Institute of Nuclear Sciences [grant nos. 451-03-68/2022-14/200019; 451-03-68/2022-14/200161 and 451-03-1/2022-14/200017].

Auauthor contributions

Andrea Pirković, Vesna Lazić: Conceptualization, Methodology, Investigation, Writing-Original draft preparation. Dijana Topalović, Sanja Kuzman, Jelena Antić-Stanković, Dragana Božić: Visualization, Data curation and analysis, Investigation. Jovan Nedeljković, Biljana Spremo-Potporević, Lada Zivković, Milica Jovanović-Krivokuća: Supervision, Writing – Reviewing and Editing.

References

- Akter M, Sikder MT, Rahman MM, et al. A systematic review on silver nanoparticles-induced cytotoxicity: physicochemical properties and perspectives. *J Adv Res* 2018;9:1–16.
- Liao C, Li Y, Tjong S. Bactericidal and cytotoxic properties of silver nanoparticles. *Int J Mol Sci* 2019;20:449.
- Miljković M, Lazić V, Davidović S, et al. Selective antimicrobial performance of biosynthesized silver nanoparticles by horse-tail extract against *E. coli*. *J Inorg Organometal Polym Mater* 2020;30:2598–607.
- Davidović S, Lazić V, Vukoje I, et al. Dextran coated silver nanoparticles — chemical sensor for selective cysteine detection. *Coll Surf B Biointerf* 2017;160:184–91.
- De Matteis V, Malvindi MA, Galeone A, et al. Negligible particle-specific toxicity mechanism of silver nanoparticles: the role of Ag⁺ ion release in the cytosol. *Nanomed Nanotechnol Biol Med*. 2015;11:731–9.
- Medina E, Romero C, García P, et al. Characterization of bioactive compounds in commercial olive leaf extracts, and olive leaves and their infusions. *Food Function* 2019;10:4716–24.
- De Matteis V, Rizzello L, Ingrosso C, et al. Cultivar-dependent anticancer and antibacterial properties of silver nanoparticles synthesized using leaves of different olea europaea trees. *Nanomaterials* 2019;9:1544.
- Rashidipour M, Heydari R. Biosynthesis of silver nanoparticles using extract of olive leaf: synthesis and in vitro cytotoxic effect on MCF-7 cells. *J Nanostruct Chem* 2014;4:112.
- Juven B, Henis Y. Studies on the antimicrobial activity of olive phenolic compounds. *J Appl Bacteriol* 1970;33:721–32.
- Aziz NH, Farag SE, Mousa LA, et al. Comparative antibacterial and antifungal effects of some phenolic compounds. *Microbios* 1998;93:43–54.
- Furneri PM, Marino A, Saija A, et al. In vitro antimycoplasmal activity of oleuropein. *Int J Antimicrob Agents* 2002;20:293–6.
- Bisignano G, Tomaino A, Cascio RL, et al. On the in-vitro antimicrobial activity of oleuropein and hydroxytyrosol. *J Pharm Pharmacol* 2010;51:971–4.
- Caruso D, Berra B, Giavarini F, et al. Effect of virgin olive oil phenolic compounds on in vitro oxidation of human low density lipoproteins. *Nutr Metabol Cardiovas Dis* 1999;9:102–7.
- Benavente-García O, Castillo J, Lorente J, et al. Antioxidant activity of phenolics extracted from *Olea europaea* L. leaves. *Food Chem* 2000;68:457–62.
- Ziogas V, Tanou G, Molassiotis A, et al. Antioxidant and free radical-scavenging activities of phenolic extracts of olive fruits. *Food Chem* 2010;120:1097–103.
- Markhali FS, Teixeira JA, Rocha CMR. Olive tree leaves—a source of valuable active compounds. *Processes* 2020;8:1177.
- El-Gogary RI, Ragai MH, Moftah N, et al. Oleuropein as a novel topical antipsoriatic nutraceutical: formulation in microemulsion nanocarrier and exploratory clinical appraisal. *Expert Opin Drug Deliv* 2021;18:1523–32.
- Nediani C, Ruzzolini J, Romani A, et al. Oleuropein, a bioactive compound from *Olea europaea* L., as a potential preventive and therapeutic agent in non-communicable diseases. *Antioxidants* 2019;8:578.
- Genc N, Yildiz I, Chaoui R, et al. Biosynthesis, characterization and antioxidant activity of oleuropein-mediated silver nanoparticles. *Inorg Nano-Metal Chem* 2021;51:411–9.
- Ghobashy MM, Elkodous MA, Shabaka SH, et al. An overview of methods for production and detection of silver nanoparticles, with emphasis on their fate and toxicological effects on human, soil, and aquatic environment. *Nanotechnol Rev* 2021;10:954–77.
- Campagnolo L, Massimiani M, Vecchione L, et al. Silver nanoparticles inhaled during pregnancy reach and affect the placenta and the foetus. *Nanotoxicology* 2017;11:687–98.
- Zhang J, Liu S, Han J, et al. On the developmental toxicity of silver nanoparticles. *Mater Design* 2021;203:109611.
- Fry RC, Bangma J, Szilagyi J, et al. Developing novel in vitro methods for the risk assessment of developmental and placental toxicants in the environment. *Toxicol Appl Pharmacol* 2019;378:114635.
- Vuković B, Milić M, Dobrošević B, et al. Surface stabilization affects toxicity of silver nanoparticles in human peripheral blood mononuclear cells. *Nanomaterials* 2020;10:1390.
- Ilić V, Šaponjić Z, Vodnik V, et al. The influence of silver content on antimicrobial activity and color of cotton fabrics functionalized with Ag nanoparticles. *Carbohydr Polymers* 2009;78:564–9.
- Čabarkapa A, Živković L, Žukovec D, et al. Protective effect of dry olive leaf extract in adrenaline induced DNA damage evaluated using in vitro comet assay with human peripheral leukocytes. *Toxicol Vitro*. 2014;28:451–6.
- Møller P, Azqueta A, Boutet-Robinet E, et al. Minimum Information for Reporting on the Comet Assay (MIRCA): recommendations for describing comet assay procedures and results. *Nat. Protoc* 2020;15:3817–26.
- Collins AR, Dusinská M, Gedik CM, et al. Oxidative damage to DNA: do we have a reliable biomarker? *Environ Health Persp* 1996;104:465–9.
- Kelly KL, Coronado E, Zhao LL, et al. The optical properties of metal nanoparticles: the influence of size, shape, and dielectric environment. *J Phys Chem B* 2003;107:668–77.
- Huang T, Xu X-HN. Synthesis and characterization of tunable rainbow colored colloidal silver nanoparticles using single-nanoparticle plasmonic microscopy and spectroscopy. *J Mater Chem* 2010;20:9867–76.
- Gentile L, Uccella N, Sivakumar G. Soft-MS and computational mapping of oleuropein. *Int J Mol Sci* 2017;18:992.
- Khalil MMH, Ismail EH, El-Baghdady KZ, et al. Green synthesis of silver nanoparticles using olive leaf extract and its antibacterial activity. *Arab J Chem* 2014;7:1131–9.
- Rolim WR, Pelegrino MT, de Araújo Lima B, et al. Green tea extract mediated biogenic synthesis of silver nanoparticles: characterization, cytotoxicity evaluation and antibacterial activity. *Appl Surf Sci* 2019;463:66–74.
- Vukovic VV, Nedeljkovic JM. Surface modification of nanometer-scale silver particles by imidazole. *Langmuir* 1993;9:980–3.
- Bankura KP, Maity D, Mollick MMR, et al. Synthesis, characterization and antimicrobial activity of dextran stabilized silver nanoparticles in aqueous medium. *Carbohydr Polym* 2012;89:1159–65.

36. Rai M, Yadav A, Gade A. Silver nanoparticles as a new generation of antimicrobials. *Biotechnol Adv* 2009;27:76–83.
37. Vazquez-Muñoz R, Borrego B, Juárez-Moreno K, et al. Toxicity of silver nanoparticles in biological systems: does the complexity of biological systems matter? *Toxicol Lett* 2017;276:11–20.
38. Panáček A, Kvítek L, Pucek R, et al. Silver colloid nanoparticles: synthesis, characterization, and their antibacterial activity. *J Phys Chem B* 2006;110:16248–53.
39. SL M, VM E. Cytotoxicity in MCF-7 and MDA-MB-231 breast cancer cells, without harming MCF-10A healthy cells. *J Nanomed Nanotechnol* 2016;07:369.
40. Ruiz-Ruiz B, Arellano-García ME, Radilla-Chávez P, et al. Cytokinesis-block micronucleus assay using human lymphocytes as a sensitive tool for cytotoxicity/genotoxicity evaluation of AgNPs. *ACS Omega* 2020;5:12005–15.
41. Greulich C, Diendorf J, Geßmann J, et al. Cell type-specific responses of peripheral blood mononuclear cells to silver nanoparticles. *Acta Biomaterialia* 2011;7:3505–14.
42. Jiang X, Miclăuş T, Wang L, et al. Fast intracellular dissolution and persistent cellular uptake of silver nanoparticles in CHO-K1 cells: implication for cytotoxicity. *Nanotoxicology* 2015;9:181–9.
43. Choi Y-J, Park J-H, Han J, et al. Differential cytotoxic potential of silver nanoparticles in human ovarian cancer cells and ovarian cancer stem cells. *Int J Mol Sci* 2016;17:2077.
44. Malysheva A, Ivask A, Doolette CL, et al. Cellular binding, uptake and biotransformation of silver nanoparticles in human T lymphocytes. *Nat Nanotechnol* 2021;16:926–32.
45. Jovanović M, Stefanoska I, Radojčić L, et al. Interleukin-8 (CXCL8) stimulates trophoblast cell migration and invasion by increasing levels of matrix metalloproteinase (MMP)2 and MMP9 and integrins $\alpha 5$ and $\beta 1$. *Reproduction* 2010;139:789–98.
46. Stefanoska I, Jovanović Krivokuća M, Vasilijić S, et al. Prolactin stimulates cell migration and invasion by human trophoblast in vitro. *Placenta* 2013;34:775–83.
47. Jovanović Krivokuća M, Stefanoska I, Abu Rabi T, et al. Pharmacological inhibition of MIF interferes with trophoblast cell migration and invasiveness. *Placenta* 2015;36:150–9.
48. Costa IN, Ribeiro M, Silva Franco P, et al. Biogenic silver nanoparticles can control toxoplasma gondii infection in both human trophoblast cells and villous explants. *Front Microbiol* 2021;11:623947.
49. Oberdörster G, Oberdörster E, Oberdörster J. Nanotoxicology: an emerging discipline evolving from studies of ultrafine particles. *Environ Health Perspect* 2005;113:823–39.
50. Riaz M, Mutreja V, Sareen S, et al. Exceptional antibacterial and cytotoxic potency of monodisperse greener AgNPs prepared under optimized pH and temperature. *Sci Rep* 2021;11:2866.
51. Abdal Dayem A, Hossain M, Lee S, et al. The Role of Reactive Oxygen Species (ROS) in the biological activities of metallic nanoparticles. *Int J Mol Sci* 2017;18:120.
52. Schins RPF. Mechanisms of genotoxicity of particles and fibers. *Inhal Toxicol* 2002;14:57–78.
53. Dayem AA, Kim B, Gurunathan S, et al. Biologically synthesized silver nanoparticles induce neuronal differentiation of SH-SY5Y cells via modulation of reactive oxygen species, phosphatases, and kinase signaling pathways. *Biotechnol J* 2014;9:934–43.
54. Guo X, Li Y, Yan J, et al. Size- and coating-dependent cytotoxicity and genotoxicity of silver nanoparticles evaluated using in vitro standard assays. *Nanotoxicology* 2016;10:1373–84.
55. Huk A, Izak-Nau E, el Yamani N, et al. Impact of nanosilver on various DNA lesions and HPRT gene mutations—effects of charge and surface coating. *Particle Fibre Toxicol* 2015;12:25.
56. Butler KS, Peeler DJ, Casey BJ, et al. Silver nanoparticles: correlating nanoparticle size and cellular uptake with genotoxicity. *Mutagenesis* 2015;30:577–91.
57. Lebedová J, Hedberg YS, Odnevall Wallinder I, et al. Size-dependent genotoxicity of silver, gold and platinum nanoparticles studied using the mini-gel comet assay and micronucleus scoring with flow cytometry. *Mutagenesis* 2018;33:77–85.
58. Joksić G, Stašić J, Filipović J, et al. Size of silver nanoparticles determines proliferation ability of human circulating lymphocytes in vitro. *Toxicol Lett* 2016;247:29–34.
59. Koklesova L, Liskova A, Samec M, et al. Genoprotective activities of plant natural substances in cancer and chemopreventive strategies in the context of 3P medicine. *EPMA J* 2020;11:261–87.
60. Topalović D, Dekanski D, Spremo-Potparević B, et al. Dry olive leaf extract attenuates DNA damage induced by estradiol and diethylstilbestrol in human peripheral blood cells in vitro. *Mutat Res Toxicol Environ Mutagen* 2019;845:402993.
61. Zorić N, Kopjar N, Rodriguez JV, et al. Protective effects of olive oil phenolics oleuropein and hydroxytyrosol against hydrogen peroxide-induced DNA damage in human peripheral lymphocytes. *Acta Pharm* 2021;71:131–41.
62. Auer GK, Weibel DB. Bacterial cell mechanics. *Biochemistry* 2017;56:3710–24.
63. Zorić N, Kosalec I. The Antimicrobial Activities of Oleuropein and Hydroxytyrosol. In: Rai, M., Kosalec, I. (eds.) Promising Antimicrobials from Natural Products, Chapter V. Cham: Springer, 2022, 75-89.
64. Tripoli E, Giammanco M, Tabacchi G, et al. The phenolic compounds of olive oil: structure, biological activity and beneficial effects on human health. *Nutr Res Rev* 2005;18:98–112.